

Experimental report

25/01/2022

Proposal: 4-02-592

Council: 4/2020

Title: Enhancement of magnetic critical scattering and nematic spin correlations in uniaxial strained Ba(Fe_{0.975}Co_{0.025})₂As₂ (TS=103K, TN=98K)

Research area: Physics

This proposal is a continuation of 4-02-531

Main proposer: Xingye LU

Experimental team: Mechthild ENDERLE
Long TIAN

Local contacts: Mechthild ENDERLE
Ursula Benggaard HANSEN

Samples: Ba(Fe_{0.975}Co_{0.025})₂As₂

Instrument	Requested days	Allocated days	From	To
IN20	0	6	15/02/2021	22/02/2021
IN22	8	0		

Abstract:

A small in-plane external uniaxial pressure has been widely used as an effective method to acquire single domain iron pnictides, it can also serve as an effective symmetry breaking field in the study of in-plane electronic nematic in underdoped samples. In our previous polarized neutron scattering experiments on unstrained BaFe₂As₂, the longitudinal mode (M_a) dominates the low-energy spin fluctuations and diverges at TN, while the transverse modes (M_b , M_c) evolve smoothly and change less across TN. However, based on our latest result on BaFe₂As₂ with uniaxial pressure, not only the longitudinal mode M_a diverges, but the transverse mode M_c perpendicular to the applied uniaxial strain also exhibits a clear diverging behavior, indicating uniaxial strain induce a c-axis magnetic moment, or simply affect the magnetic critical scattering. Because the enhancement of M_c indicates that similar electronic nematic materials may offer a novel route for magneto-mechanical control, we proposal study the underlying origin and its connection to electronic nematic with polarized neutron on underdoped Ba(Fe_{0.975}Co_{0.025})₂As₂, where the nematic reaches a maximum and the TS and TN are well separated.

Enhancement of magnetic critical scattering and nematic spin correlations in uniaxial strained $\text{Ba}(\text{Fe}_{0.974}\text{Co}_{0.026})_2\text{As}_2$

A small in-plane external uniaxial pressure has been widely used as an effective method to acquire single domain iron pnictide[1]. In our previous polarized neutron scattering experiments on unstrained and strained BaFe_2As_2 , the transverse modes Mc together with the longitudinal mode (Ma) at $E = 2\text{meV}$ dominates the low-energy spin fluctuations and diverges at T_N in the strained samples, indicating uniaxial strain could induce a c-axis magnetic moment, or simply affect the magnetic critical scattering[2, 3]. The three magnetic excitation components of strained sample represent the structure of nematic spin correlations in spin space, and the anisotropy should be even stronger in $\text{Ba}(\text{Fe}_{0.975}\text{Co}_{0.025})_2\text{As}_2$ where electronic nematic reach a maximum. Furthermore, the phase transition temperatures (T_S and T_N) are well separated in this doping ($\approx 5\text{K}$), which will provide us a clearer information about the diverging temperature, and could be a more appropriate candidate to enable us to understand the underlying origin of the magneto-mechanical control and its possible connection to electronic nematic. We got 8 days' beamtime on IN20 to study this issue.

The basic information for the sample and polarized neutron scattering experiment

Fig.1 (c) shows the samples and device we used during this experiment, 12 pieces of squared samples were mounted onto the device with uniaxial pressure applied along the b axis of orthorhombic phase. The total mass of the samples are about 2.7g. The lattice parameter we used during this experiment are $a = 5.631\text{\AA}$, $b = 5.571\text{\AA}$, $c = 13.01\text{\AA}$. The scattering plane is (H,0,L), and the energy of the incident neutron is 14.7meV , corresponding to the wave length 2.662\AA .

Fig.1 (a) and (b) show the results of transport measurements I carried on this sample, we can get the $T_N \approx 92\text{K}$ and $T_S \approx 98\text{K}$ from the Fig.1(a), which were measured without pressure. Fig.1(b) shows the anisotropy of temperature dependence of the in-plane resistance with uniaxial pressure applied along b axis, the ρ_a and ρ_b separate from each at a temperature of $T^* \approx 220\text{K}$. We can also find the T_N with the uniaxial pressure applied on the samples is about 103K from Fig.1(b).

Elastic data analysis

Fig.2 (a)-(b) show the raw data of the temperature dependence of the order parameter for three channels, the T_N increase to about 102K after applying the uniaxial pressure. Based on the equation below, we can get the information between $(\sigma_x^{\text{SF}}(\mathbf{Q}) - \sigma_y^{\text{SF}}(\mathbf{Q}))$ or $(\sigma_z^{\text{SF}}(\mathbf{Q}) - \sigma_y^{\text{SF}}(\mathbf{Q}))$ and Ma, Mc. Shown in the Fig.2 (d), we can find a relatively strong peak at about 102K from the $(\sigma_z^{\text{SF}}(\mathbf{Q}) - \sigma_y^{\text{SF}}(\mathbf{Q}))$ cure.

$$\begin{cases} \sigma_x^{\text{SF}}(\mathbf{Q}) = F^2(\mathbf{Q}) \sin^2 \alpha_{\mathbf{Q}} \frac{R}{R+1} M_a + F^2(\mathbf{Q}) \frac{R}{R+1} M_b + F^2(\mathbf{Q}) \cos^2 \alpha_{\mathbf{Q}} \frac{R}{R+1} M_c + B(\mathbf{Q}) \\ \sigma_y^{\text{SF}}(\mathbf{Q}) = F^2(\mathbf{Q}) \sin^2 \alpha_{\mathbf{Q}} \frac{1}{R+1} M_a + F^2(\mathbf{Q}) \frac{R}{R+1} M_b + F^2(\mathbf{Q}) \cos^2 \alpha_{\mathbf{Q}} \frac{1}{R+1} M_c + B(\mathbf{Q}) \\ \sigma_z^{\text{SF}}(\mathbf{Q}) = F^2(\mathbf{Q}) \sin^2 \alpha_{\mathbf{Q}} \frac{R}{R+1} M_a + F^2(\mathbf{Q}) \frac{1}{R+1} M_b + F^2(\mathbf{Q}) \cos^2 \alpha_{\mathbf{Q}} \frac{R}{R+1} M_c + B(\mathbf{Q}) \end{cases} \quad (1)$$

$$\begin{cases} \sigma_z^{\text{SF}}(\mathbf{Q}_1) - \sigma_y^{\text{SF}}(\mathbf{Q}_1) = \frac{R-1}{R+1} F^2(\mathbf{Q}_1) [\sin^2 \alpha_1 M_a + \cos^2 \alpha_1 M_c - M_b] \propto 0.16 M_a + 0.84 M_c - M_b \\ \sigma_z^{\text{SF}}(\mathbf{Q}_2) - \sigma_y^{\text{SF}}(\mathbf{Q}_2) = r \frac{R-1}{R+1} F^2(\mathbf{Q}_2) [\sin^2 \alpha_2 M_a + \cos^2 \alpha_2 M_c - M_b] \propto 0.63 M_a + 0.37 M_c - M_b \\ \sigma_x^{\text{SF}}(\mathbf{Q}_1) - \sigma_y^{\text{SF}}(\mathbf{Q}_1) = \frac{R-1}{R+1} F^2(\mathbf{Q}_1) [\sin^2 \alpha_1 M_a + \cos^2 \alpha_1 M_c] \propto 0.16 M_a + 0.84 M_c \\ \sigma_x^{\text{SF}}(\mathbf{Q}_2) - \sigma_y^{\text{SF}}(\mathbf{Q}_2) = r \frac{R-1}{R+1} F^2(\mathbf{Q}_2) [\sin^2 \alpha_2 M_a + \cos^2 \alpha_2 M_c] \propto 0.63 M_a + 0.37 M_c \end{cases} \quad (2)$$

Fig.3 shows the background signal (BG) subtracted $\theta-2\theta$ scans at 80K , 100K , 105K , 107K and 130K at (101) and (103) positions. We can see the intensity of the elastic peaks at 105K and 107K reduce a little more at (103) compared with (101), since σ_x and σ_z shows different combination of Ma and Mc at these two positions, the different change of the intensity at 105K and 107K between (101) and (103) indicate the change of Ma and Mc at these temperatures.

Inelastic data analysis

The spin flipping ratio R chosen to use is 22.6, which is the average of the $[\text{R}_x, \text{R}_y, \text{R}_z] = [22.9286, 19.1250, 25.6415]$, these values is measured at the (200) nuclear Bragg peak at 130K . The parameter r in equation (2) was solved by the inelastic energy scans data at 80K , 100K , 120K and the temperature dependence of the spin excitation with $E_T = 2\text{meV}$, its value of 1.1 is applied by taking into account of the fitting results, the analysing procedure is described in the previous work of our group[4].

Fig.4 shows the results of energy scans at 80K , 100K and 120K with all three channels. Fig.4 (a)(b)(c) show the $\sigma_z^{\text{SF}} - \sigma_y^{\text{SF}}$ at (101) and (103), because of $\sigma_z^{\text{SF}} - \sigma_y^{\text{SF}} \propto M_y - M_b$, and $M_y = \sin^2 \alpha M_a + \cos^2 \alpha M_c$, M_b does not diverge at T_N , $\sigma_z^{\text{SF}} - \sigma_y^{\text{SF}}$ can be a good reference to probe Mc. As it diverge only the at 100K below about 6.5meV , thus unambiguously confirming that the uniaxial pressure-induced Mc is enhanced at around T_N . Fig. 4 (d)(e)(f) show the temperature dependence of the magnetic moment extracted from the above energy scans. At 100K , Ma and Mb are

gapped below about 8meV and 5meV, respectively; at 100K, we see the enhancement of Ma and Mc below about 5 meV; at 120K, there is no magnetic signal.

Fig.5 (a)(b) show the temperature dependence of the σ_x^{SF} , σ_y^{SF} and σ_z^{SF} at E=2meV. Since σ_z is sensitive to Mc at (101), we see a clear diverge of σ_z^{SF} , which indicates the strain enhanced Mc near 100K. Fig.7 (c) shows the temperature dependence of $\sigma_z^{\text{SF}} - \sigma_y^{\text{SF}}$, its divergence can again confirm the enhancement of Mc at T_N . Fig.7 (d) shows the temperature dependence of Ma, Mb and Mc, we can see both Ma and Mc diverge at T_N .

Calculate the magnetic ordered moment

The calculation process is mainly completed by using the magnetic Bragg peaks at (101), (103) and the nuclear Bragg peak at (200). The detailed procession can be find in the "calculate ordered moment" file.

The ordered moment I get at 2K is $0.1823\mu\text{B}$ ($x = 0.026$, $T_N \approx 92\text{K}$ without pressure and 100K with pressure), compared with $0.49\mu\text{B}$ ($x=0.021$, $T_N \approx 105\text{K}$), $0.25\mu\text{B}$ ($x=0.022$, $T_N \approx 100\text{K}$) and $0.31\mu\text{B}$ ($x=0.39$, $T_N \approx 66\text{K}$) of the twinned sample.

The ordered moment I get at 100K are $m_a = 0.0443\mu\text{B}$ and $m_c = 0.0127\mu\text{B}$. The canting angle should be $\alpha = \arctan(\frac{m_c}{m_a}) \approx 16.8^\circ$.

The ordered moment I get at 120K are small, $m_a = 0.0073\mu\text{B}$ and $m_c = 0.0033\mu\text{B}$.

References

- [1] R. M. Fernandes et al., Nat. Phys. **10**, 97 (2014).
- [2] Yu Li et al., Phys. Rev. B **96**, 020404(R) (2017).
- [3] Panpan Liu et al., Nat. Comm. **11**, 5728 (2020).
- [4] Chenglin Zhang et al., Phys. Rev. B **90**, 140502(R) (2014).

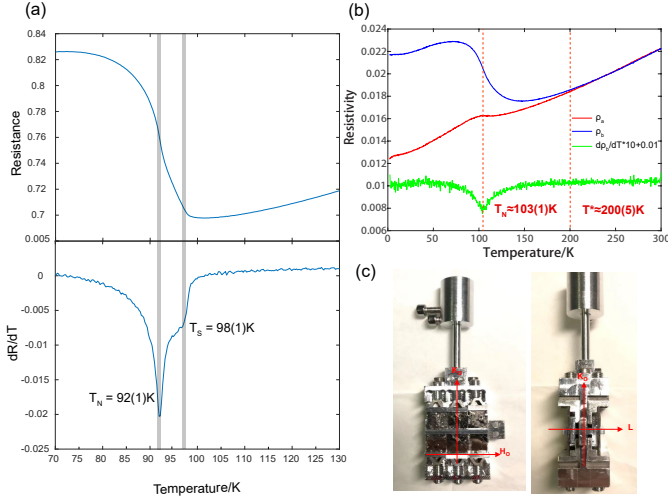


Figure 1: (a) Temperature dependence of the resistance and dR/dT , the vertical dashed lines indicate the $T_N \approx 92\text{K}$ and $T_S \approx 98\text{K}$ of the sample. (b) Temperature dependence of the resistance along a and b axes under uniaxial pressure, the green lines represent the smoothed curves for Ra and Rb. (c) Photos of the samples and device used during the experiment.

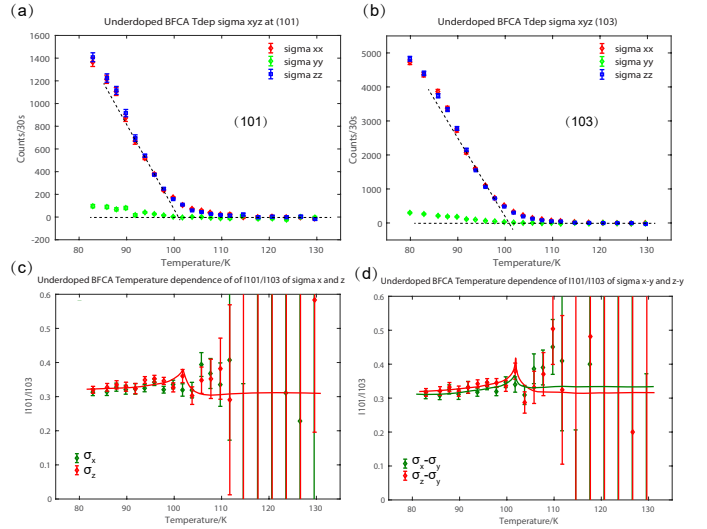


Figure 2: (a)-(b) Temperature dependence of the order parameter with all three channels at (101) and (103). (c) Temperature dependence of the ratio of I_{101} and I_{103} calculated with σ_x and σ_z . (d) Temperature dependence of the ratio of I_{101} and I_{103} calculated with $\sigma_x - \sigma_y$ and $\sigma_z - \sigma_y$.

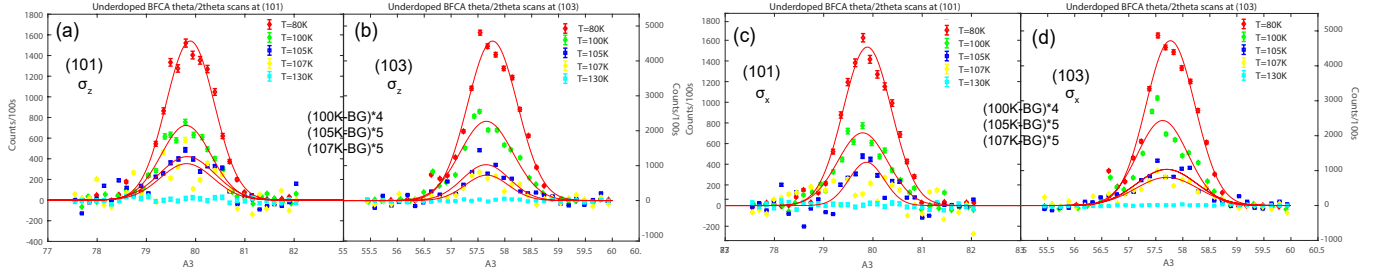


Figure 3: (a)-(b) θ - 2θ scans at (101) and (103) in SF mode for all three components at 80K, 100K, 105K, 107K and 130K extracted from σ_z , (d)-(e) the same scans extracted from σ_x .

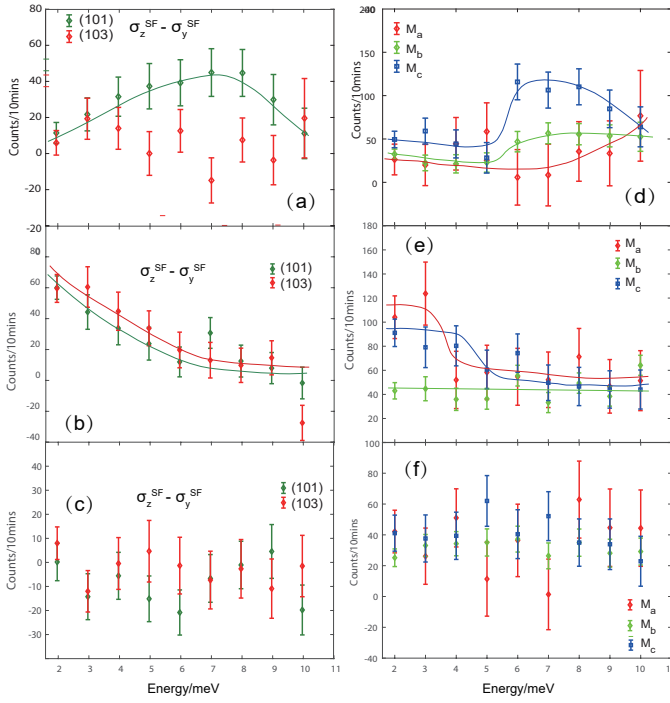


Figure 4: The energy dependence of $\sigma_z^{\text{SF}} - \sigma_y^{\text{SF}}$ at 80K (a), 100K (b) and 120K (c). The energy dependence of M_a , M_b and M_c extracted from the data at 80K (d), 100K (e) and 120K (f).

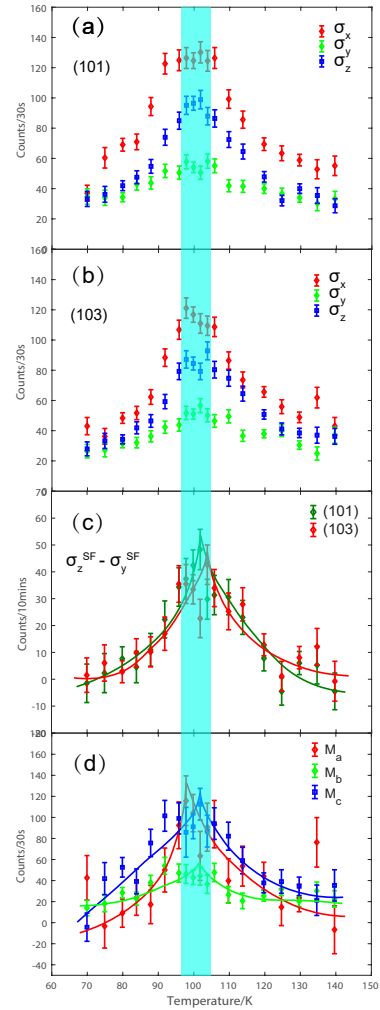


Figure 5: The temperature dependence of all three channels at (101) (a) and (103) (b). The temperature dependence of $\sigma_z^{\text{SF}} - \sigma_y^{\text{SF}}$ at (101) and (103). The temperature dependence of M_a , M_b and M_c extracted from the above data.